

Photophysical and photoconductive properties of organic semiconductor composites

Andrew D. Platt^a, Whitney E. B. Shepherd^a,
John E. Anthony^b, and Oksana Ostroverkhova^a

^aDepartment of Physics, Oregon State University, Corvallis, OR 97331, USA;
^bDepartment of Chemistry, University of Kentucky, Lexington, KY 40506, USA

ABSTRACT

We report on the effects of introducing guest molecules into a functionalized anthradithiophene (ADT) host on the photoluminescent (PL) and photoconductive properties of solution-deposited thin films. An addition of 0.1 wt % of an ADT derivative with cyano end groups (ADT-TIPS-CN) to a fluorinated ADT derivative (ADT-TES-F) resulted in the near complete quenching of the fluorescence spectrum of the ADT-TES-F host with an enhancement in the fluorescence spectrum of the ADT-TIPS-CN guest. A markedly longer PL lifetime was noted in films containing 10% ADT-TIPS-CN guest molecules compared to both pristine ADT-TES-F and ADT-TIPS-CN films. Stronger temperature dependence of the PL quantum yield was obtained in ADT-TIPS-CN/ADT-TES-F films at low ADT-TIPS-CN concentrations than in films of pristine material, with PL decreasing with increasing temperature. Significant changes in the photoexcited charge carrier dynamics were observed on nanosecond time-scales after 400 nm 100 fs pulsed photoexcitation upon adding ADT-TIPS-CN guest molecules to the ADT-TES-F host. In contrast, no considerable change in the photocurrent was detected under continuous wave 532 nm excitation for guest molecule concentrations up to 1% of ADT-TIPS-CN in ADT-TES-F.

Keywords: organic semiconductors, thin films, photoluminescence, energy transfer, photoconductivity

1. INTRODUCTION

Organic semiconductors have attracted considerable attention due to their potential applications in low-cost and/or large-area (opto)electronic devices.¹ Solution-processable materials can be tailored for specific applications by creating mixtures of various derivatives, thus tuning the optical and electronic properties of the resulting composites.² While polymer composites have been extensively studied,³ composites based on small molecular weight materials have not been explored to the same extent due to reduced solubility of many high-performance compounds, thus requiring, for example, thermal coevaporation in vacuum, which limits practical use of such composites. Recently, a variety of high-performance solution-processable functionalized pentacene and anthradithiophene (ADT) derivatives have been synthesized and characterized.^{4,5} Charge carrier mobilities over 1.2 cm²/Vs have been reported in spin-coated and drop-cast thin films of several derivatives including ADT derivatives used in our study.^{6,7} In addition, fast charge photogeneration and high bulk photoconductive gains have been observed in thin films of many derivatives, with a fluorinated ADT thin film exhibiting gains of up to 130, which is more than an order of magnitude higher than that in other organic materials under similar conditions.^{5,8-10} Finally, both highly fluorescent and non-fluorescent materials are available (e.g. functionalized ADT and pentacene derivatives, respectively).⁵

In addition to a promising potential of ADT pristine compounds for (opto)electronic applications, the availability of these high-performance, solution-processable, structurally similar, derivatives with different highest occupied molecular orbital (HOMO) and lowest unoccupied molecular orbital (LUMO) energies can be utilized to create composites with specified optical and electronic properties. Previously, we reported on the effect of introducing various guest molecules in the fluorinated ADT host (ADT-TES-F) on charge carrier dynamics at time-scales from sub-nanoseconds to tens of microseconds after a 400 nm 100 fs photoexcitation.² Especially

Further author information: (Send correspondence to O.O.)

O.O: E-mail: oksana@science.oregonstate.edu, Telephone: 1 541 737 1679

J.E.A.: E-mail: anthony@uky.edu, Telephone: 1 859 257 8844

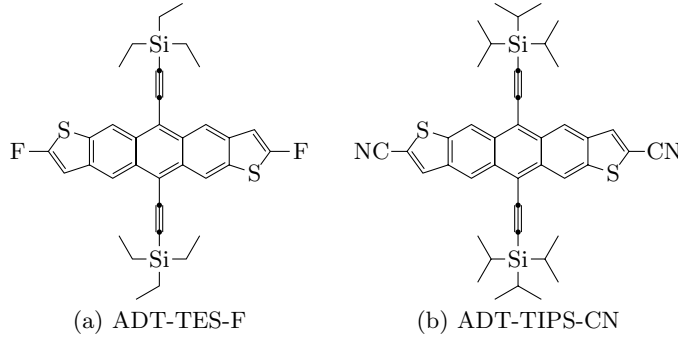


Figure 1. Anthradithiophene functionalized with side groups of (a) SiEt₃ (TES) with F end groups, ADT-TES-F, and (b) Si*i*-Pr₃ (TIPS) with end CN groups, ADT-TIPS-CN.

dramatic effects on charge photogeneration were observed upon adding a cyano-group-containing ADT derivative (ADT-TIPS-CN) to the ADT-TES-F host, which resulted in photoinduced energy transfer between the host and guest molecules.² In this paper, we examine the effects of the embedding of ADT-TIPS-CN molecules into an ADT-TES-F host on photoluminescence (PL) and photocurrent in more detail.

2. EXPERIMENTAL

2.1 Materials and Sample Preparation

In our studies, we explored thin films of a fluorinated ADT derivative functionalized with triethylsilylethynyl (TES) side groups (ADT-TES-F), both pristine and doped with various concentrations of another ADT derivative functionalized with triisopropylsilylethynyl (TIPS), ADT-TIPS-CN (Figure 1). The synthesis of these ADT derivatives (ADT-TIPS(TES)-F(CN)) has been reported elsewhere.^{5,7}

Stock solutions of functionalized ADT derivatives were prepared at $\sim 1\%$ by weight in toluene. For solution measurements, solutions were prepared by dilution of stock solutions to $\sim 10^{-4}$ M. Films with thickness of $1 - 2 \mu\text{m}$ were prepared by drop-casting stock solutions onto glass substrates at $\sim 60^\circ\text{C}$. Composite films were similarly prepared from stock solutions of known mixtures of ADT-TES-F and ADT-TIPS-CN. When dealing with pristine compounds, this preparation method yielded polycrystalline ADT-TES-F and amorphous ADT-TIPS-CN films (as confirmed by X-ray diffraction and transmission electron microscopy (TEM)).

For measurements of dark current and photoresponse, glass substrates were prepared by photolithographic deposition of either 5 nm/50 nm thick Cr/Au or 100 nm thick aluminum (Al) electrode pairs. Each pair consisted of 10 interdigitated finger pairs, with 1 mm finger length, 25 μm finger width and 25 μm gaps between the fingers of opposite electrodes. Films were drop-cast onto the interdigitated regions.

2.2 Optical Properties

Optical absorption spectra were measured using a halogen lamp and a fiber-coupled Ocean Optics USB2000 spectrometer. Absorbance A was calculated from the incident (I_0) and transmitted (I) beam intensities as $A = -\text{Log}(I/I_0)$. Reflection losses were taken into account by referencing with respect to cuvettes with pure solvent or clean glass substrates for solution and film measurements, respectively.

Emission spectra were acquired in a custom fluorescence measurement setup with laser excitation at wavelengths of either 400 nm (frequency-doubled mode-locked Ti:Sapphire laser from KM Labs) or 532 nm (Nd:YVO₄ laser from Coherent, Inc.). Emitted photons were collected using a parabolic mirror and detected with a fiber coupled spectrometer (Ocean Optics USB2000) calibrated against a 3100 K black-body emitter. Absorption of solutions was measured using a standard 1 cm path length quartz cuvette with a halogen light source fiber-optically delivered to the sample holder and spectrometer. PL quantum yields (QYs) in solution (Φ) were referenced against standards with known quantum yields and corrected for differences in optical density and

solvent refractive index.¹¹ The ADT derivatives were measured against rhodamine 6G in ethanol ($\Phi = 0.95$) and DCDHF-N-6 in toluene ($\Phi = 0.85$).¹² The detection limit of the setup was estimated to be at $\Phi \approx 0.5\%$.

PL lifetime measurements were performed using a mode-locked Ti:Sapphire laser frequency-doubled with a beta-barium borate (BBO) crystal with a repetition rate of 93 MHz picked at 9.3 MHz using a home-built pulse picker (based on a TeO₂ acousto-optic modulator from NEOS) and pulses 80 fs in length as the excitation source. A single-photon avalanche photodiode (SPAD – Molecular Photonic Devices) was used in conjunction with a time-correlated single-photon counter (TCSPC) data analysis board (PicoQuant TimeHarp 200) for detection. The instrument response function (IRF) (~ 200 ps) was recorded using scattered light from an etched microscope slide.

For measurements of the temperature dependence of film spectra, samples on pre-cut microscope slides were mounted on a custom built electrically heated and water cooled stage (range: 278 – 360 K) for temperature control. Photoluminescence measurements were taken in situ over the entire temperature range, in ambient air. Similar experiments were previously performed under N₂ atmosphere and showed no discernable difference.⁵

2.3 Dark current, transient and cw photocurrent measurements

For transient photocurrent measurements, an amplified Ti:Sapphire laser (800 nm, 100 fs, 1 kHz) was used in conjunction with a frequency-doubling BBO crystal to excite the samples. Voltage was supplied by a Keithley 237 source-measure unit, and light pulse-induced transient photocurrent was measured with a 50 Ω load by a 50 GHz CSA8200 digital sampling oscilloscope.^{2,8} Average electric field E was calculated as $E = V/L$, where V is the applied voltage, and L is the gap between the electrodes. In dark current and cw photocurrent measurements, the Keithley 237 source-measure unit was used to measure current through the sample in the absence and in the presence of cw photoexcitation with a Nd:YVO₄ laser at 532 nm. The photocurrent was calculated as the difference between the two.

3. RESULTS AND DISCUSSION

3.1 Optical properties in solution

Table 1 summarizes various properties of pristine ADT-TES-F and ADT-TIPS-CN compounds in solution.⁵ Absorption spectra of these compounds in toluene solution had similar shapes that are characterized by a dominant 0 \rightarrow 0 transition and vibronic progression.⁵ Both absorption and PL spectra of the ADT-TIPS-CN in toluene are redshifted with respect to those of the ADT-TES-F by ~ 55 nm (Fig. 2 (a) and (b), respectively). Both compounds are highly fluorescent in solution, exhibiting PL quantum yields Φ of 70 and 76% in the case of ADT-TES-F and ADT-TIPS-CN, respectively.⁵ Time-resolved PL decay observed in solutions under 80 fs 400 nm pulsed excitation could be described by a single-exponential function, with a lifetime τ of 9.4 and 12.7 ns for the ADT-TES-F and ADT-TIPS-CN, respectively (Fig. 4). Upon addition of ADT-TIPS-CN molecules to ADT-TES-F in toluene solution, no ground-state charge transfer was observed since the absorption spectra of the resulting mixtures in solution were simple additions of those of the constituents (Fig. 2(a)). The PL spectra were dominated by those of the ADT-TES-F (Fig 2(b)). No PL spectral shift was observed up to at least 10% of ADT-TIPS-CN in the ADT-TIPS-CN/ADT-TES-F mixture in toluene. Reduction in the overall PL intensity, however, was observed at a level of higher than $\sim 1\%$ of ADT-TIPS-CN, in part due to slightly reduced absorption at the excitation wavelength of 532 nm.

Table 1. **Electrochemical, optical, and photoluminescent properties of ADT-TES-F and ADT-TIPS-CN derivatives in solution.**

Name	HOMO ^a (eV)	LUMO ^a (eV)	λ_{abs}^b (nm)	λ_{em}^c (nm)	Φ^d	τ^d (ns)
ADT-TES-F	-5.35	-3.05	528	536	0.70	9.4
ADT-TIPS-CN	-5.55	-3.49	582	590	0.76	12.7

- a Measured by differential pulse voltammetry⁵
b Wavelength of maximal absorption, which corresponds to 0 \rightarrow 0 transition
c Wavelength of maximal emission, which corresponds to 0 \rightarrow 0 transition
d Measured as described in Section 2.

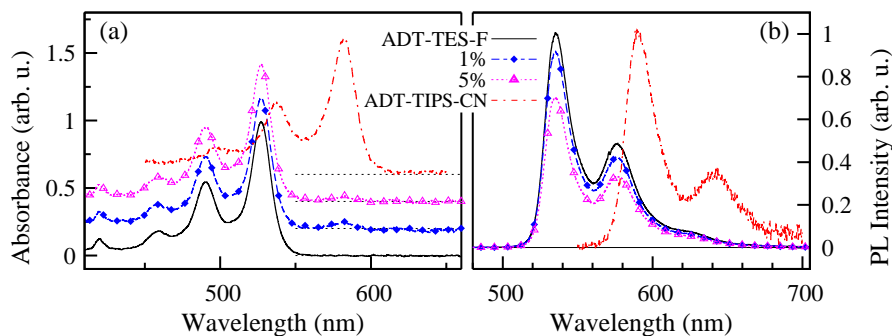


Figure 2. Absorption (a) and photoluminescence (b) spectra of toluene solutions of the ADT-TIPS-CN and ADT-TES-F mixtures at 0%, 1% and 5% concentrations of ADT-TIPS-CN with respect to ADT-TES-F. Spectra of pristine ADT-TIPS-CN in toluene solution are also shown. Absorption spectra are shifted along the y-axis for clarity. In (b), the PL spectra of ADT-TIPS-CN/ADT-TES-F mixtures are normalized by the peak value measured in pristine ADT-TES-F in toluene.

3.2 Optical properties in film

Absorption and PL spectra of pristine ADT-TES-F and ADT-TIPS-CN films were broadened and redshifted with respect to those of the same compounds in solution (Fig. 3) due to intermolecular interactions and exciton delocalization.^{5,13} These mechanisms were confirmed by our measurements of the spectra of low concentration of ADT-TES-F molecules embedded in the poly(methyl-methacrylate) (PMMA) film, which were identical to those of ADT-TES-F in solution in Fig. 2, as expected in the case of non-interacting molecules. Based on the absorption spectra in Fig. 3(a), no ground state charge transfer occurs upon adding ADT-TIPS-CN molecules into the ADT-TES-F host at the concentrations of 0.1-10% used in our study. PL spectra and quantum yields of pristine ADT-TES-F films depended somewhat on film morphology and crystallinity.⁵ However, most of our ADT-TES-F films were highly fluorescent, exhibiting quantum yields of 40-50%. In contrast to absorption spectra and PL spectra in solution, addition of the ADT-TIPS-CN molecules to ADT-TES-F in film produced a dramatic effect on the PL spectra (Fig. 3(b)). In particular, even at a concentration of ADT-TIPS-CN in ADT-TES-F as low as 0.1%, only a weak PL emission was observed from the ADT-TES-F host (peaked at \sim 625 nm), and the PL response of the film was dominated by that of the ADT-TIPS-CN guest molecules. This suggests efficient energy transfer from the photoexcited ADT-TES-F host to the ADT-TIPS-CN guest. At concentrations of ADT-TIPS-CN of 1% and higher, the PL measured in the ADT-TIPS-CN/ADT-TES-F film was solely due to ADT-TIPS-CN molecules. The PL spectrum did not significantly change upon further increase in the ADT-TIPS-CN concentration, at least up to 10%. Nevertheless, it is possible that an increase in concentration beyond 10% would lead to a significant change in molecular packing and, therefore, optical properties, since the PL spectra of the ADT-TIPS-CN/ADT-TES-F mixtures in Fig. 3(b) differed from that of

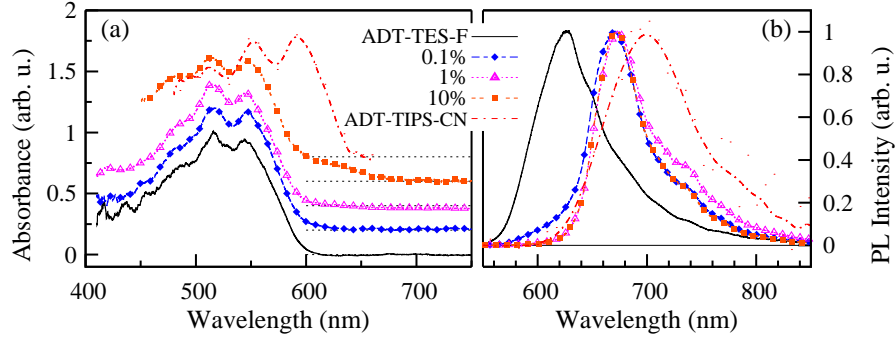


Figure 3. (a) Optical absorption and (b) PL spectra of pristine ADT-TES-F film or ADT-TIPS-CN/ADT-TES-F films with ADT-TIPS-CN levels of 0.1%, 1%, and 10%. Absorption spectra are shifted along the y-axis for clarity. The spectra of a ADT-TIPS-CN film are shown for reference.

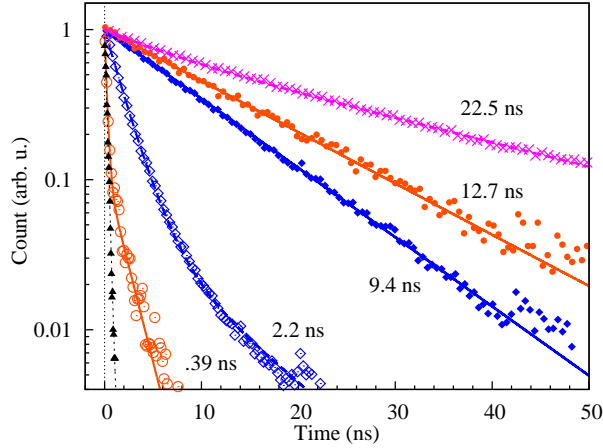


Figure 4. Normalized PL decays measured in solutions of ADT-TES-F (●) and ADT-TIPS-CN (◆), fitted with a single-exponential function $\sim \exp[-t/\tau]$. Also shown are PL decay dynamics obtained in a polycrystalline ADT-TES-F film (◇) and an amorphous ADT-TIPS-CN film (○). The films are fitted with a bi-exponential function $\sim a_1 \exp[-t/\tau_1] + a_2 \exp[-t/\tau_2]$ giving averaged lifetimes of 0.39 ns, and 2.2 ns for ADT-TIPS-CN and ADT-TES-F films, respectively. The averaged lifetime is given by $\tau_{\text{avg}} = a_1 \cdot \tau_1 + a_2 \cdot \tau_2$ where a_1 and a_2 are the normalized amplitude coefficients. Also shown is the data obtained from the ADT-TIPS-CN/ADT-TES-F film at 10% ADT-TIPS-CN fitted with a bi-exponential function with τ_{avg} of 22.5 ns (×). The instrument response function (IRF) (▲), with the full-width at half-maximum of ~ 200 ps is also included.

the pristine ADT-TIPS-CN film (also shown in Fig. 3(b)) due to differences in properties of molecular aggregates (e.g. size and packing), responsible for PL in these materials.¹⁴

In pristine ADT-TES-F and ADT-TIPS-CN films, the PL decay dynamics were faster than those in solution and could be described by a bi-exponential function ($\sim a_1 \exp[-t/\tau_1] + a_2 \exp[-t/\tau_2]$, where $\tau_{1(2)}$ and $a_{1(2)}$ are shorter (longer) lifetimes and their relative amplitudes, $a_1 + a_2 = 1$, respectively), characteristic of molecular aggregates (Figure 4).¹⁴ Both τ_1 and τ_2 were shorter than lifetimes τ measured in solutions of the same molecules and were similar for the emission at all wavelengths within the PL emission spectrum. The weighted average lifetimes in films, $\tau_{\text{av}} = a_1 \tau_1 + a_2 \tau_2$, were typically on the order of 2 and 0.4 ns for pristine ADT-TES-F and ADT-TIPS-CN films, respectively, at room temperature, and varied slightly with film quality. Interestingly, addition of ADT-TIPS-CN molecules in the ADT-TES-F host drastically changed the PL decay dynamics in films. For example, at 10% of ADT-TIPS-CN, a bi-exponential decay characterized by an average lifetime of ~ 22.5 ns was observed. This is much longer than lifetimes obtained in any pristine ADT film and/or solution studied, which suggests that solid-state interaction between ADT-TIPS-CN and ADT-TES-F molecules stabilizes the excited state while removing fast relaxation pathways. As we discuss below, this is correlated with photoconductive properties of the same sample on nanosecond time-scales after a pulsed 80 fs excitation.

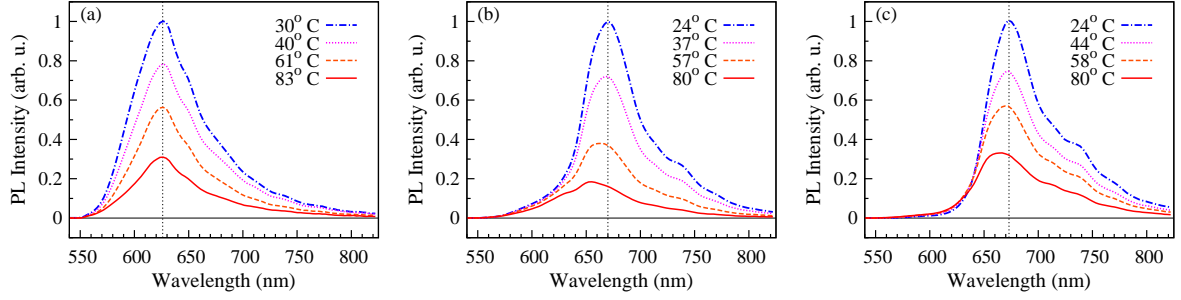


Figure 5. Characteristic PL for a pristine ADT-TES-F film (a) and ADT-TIPS-CN/ADT-TES-F composite films at ADT-TIPS-CN concentration of 0.1% (b) and 1% (c), at several temperatures.

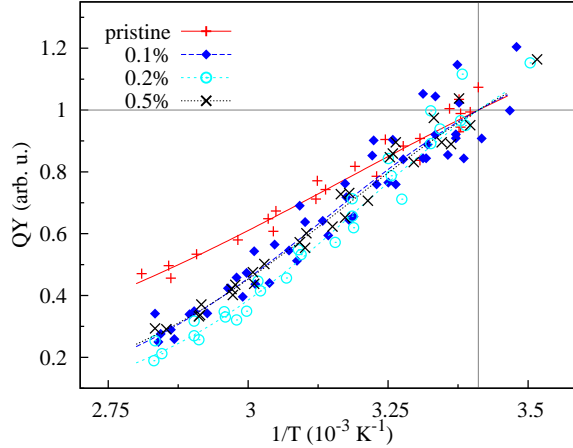


Figure 6. Relative PL quantum yield (normalized to 20 °C) for the pristine ADT-TES-F film and ADT-TIPS-CN/ADT-TES-F films at 0.1%, 0.2%, and 0.5% wt % concentrations of ADT-TIPS-CN. The temperature dependence appears stronger in composites than in pristine films.

Temperature dependence of photoluminescence. Figure 5 illustrates PL spectra of a pristine ADT-TES-F film, as well as of ADT-TIPS-CN/ADT-TES-F films at ADT-TIPS-CN concentrations of 0.1 and 1%, at various temperatures. In all films, the PL response was strongly temperature dependent, and PL quantum yields decreased by a factor of 3 – 6 as the temperature increased from 5 °C to 80 °C, depending on the sample and on the mixture (Fig. 6). Since no temperature dependence of PL emission of our molecules in solution was observed, the strong temperature dependence observed in films is due to temperature-dependent intermolecular interaction in films.^{15–18} In order to quantify the observed temperature dependence, we consider PL quantum yield to be inversely proportional to a sum of temperature independent radiative rate and thermally activated non-radiative rate,^{19,20} so that

$$1/\Phi \sim 1 + a \exp \left[\frac{-\Delta_{fl}}{k_B T} \right], \quad (1)$$

where k_B is the Boltzmann constant, T is temperature, and a is a fitting parameter related to the ratio between radiative and temperature-independent non-radiative rate prefactor. PL quenching activation energies Δ_{fl} , obtained from fits of data to Eq. 1 yielded 0.21 ± 0.05 eV in the case of the pristine ADT-TES-F and 0.38 ± 0.05 eV in the case of ADT-TIPS-CN/ADT-TES-F at ADT-TIPS-CN concentrations between 0.1 and 0.5% (Fig. 6).

Two main differences in the temperature dependence of PL between pristine ADT-TES-F and ADT-TIPS-CN/ADT-TES-F films can be noted: (i) fluorescence peak position changes, which were observed in composites, but not in the pristine ADT-TES-F films (Fig. 5), and (ii) PL quenching activation energies, which were considerably higher in composites (Fig. 6). Blueshift of the PL spectra as the temperature increased has been previously

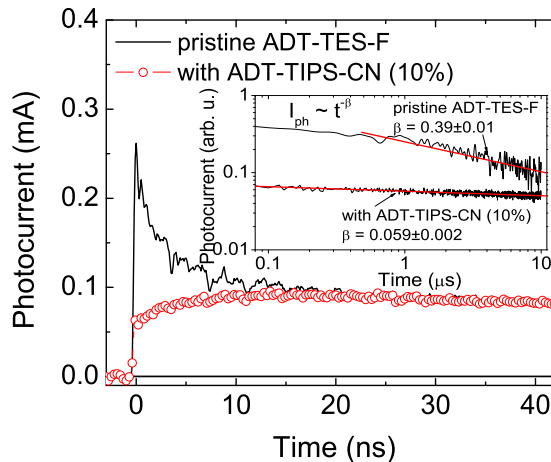


Figure 7. Transient photocurrent obtained in films of pristine ADT-TES-F and in ADT-TIPS-CN (10%)/ADT-TES-F at $5 \mu\text{J}/\text{cm}^2$ at $4 \times 10^4 \text{ V}/\text{cm}$. Inset shows photocurrent dynamics on longer time-scales.

observed in a variety of conjugated polymers^{21–23} and in perylene thin films²⁴ and attributed to temperature-dependent exciton-phonon coupling and lattice fluctuations. It is possible that since a guest ADT-TIPS-CN molecule introduced into the ADT-TES-F host disturbs π -stacking of ADT-TES-F molecules⁷ in a crystallite, it changes intermolecular coupling and introduces an additional disorder, which could lead to the observations in Figs. 5 and 6. However, further studies are needed to establish the exact mechanisms responsible for this behavior.

3.3 Transient and cw photocurrent

Transient photocurrents (due to photogenerated holes moving under applied electric field),⁸ obtained in pristine ADT-TES-F film and in the ADT-TIPS-CN/ADT-TES-F composite films at 10% of ADT-TIPS-CN (all on Au electrodes) upon 100 fs excitation at a fluence of $5 \mu\text{J}/\text{cm}^2$ at 400 nm in an electric field of $4 \times 10^4 \text{ V}/\text{cm}$ are shown in Fig. 7. In the pristine ADT-TES-F sample, the rise of the photocurrent (I_{ph}) was fast, limited by the time resolution of the setup (30 ps), and the decay dynamics were characterized by a fast initial decay component followed by a slow one that lasted up to at least 1 ms. In ADT-TES-F films, the slow decay component could be fitted with a power-law function ($I_{ph} \sim t^{-\beta}$), with $\beta=0.2-0.4$ depending on the sample.^{5,25} Addition of ADT-TIPS-CN to ADT-TES-F introduced a slow component into the photocurrent rise dynamics and completely removed the fast initial decay (Fig. 7). In particular, the fast rise of the photocurrent, limited by the time resolution of our setup, accounted only for $\sim 70\%$ of all photogenerated carriers, whereas the other 30% were generated over 0.1–20 ns. As a result, the peak of the photocurrent in the ADT-TES-F/ADT-TIPS-CN composite was achieved at about 20 ns after photoexcitation. While the fast photogeneration process does not seem to be correlated with exciton dynamics,⁵ the slow photogeneration process could be attributed to electric field-induced dissociation of the stabilized excited state observed in the same sample in our measurements of the PL decay dynamics in Fig. 6. After reaching the peak, the photocurrent exhibited a slow decay, characterized by a power-law function ($I_{ph} \sim t^{-\beta}$) with $\beta < 0.1$ (e.g. $\beta = 0.059 \pm 0.002$ in the inset of Fig. 7), which persisted to at least 1 ms after photoexcitation.² As mentioned above, our observations of complete quenching of the PL from the ADT-TES-F, while magnifying PL of the ADT-TIPS-CN (Fig. 3) in the ADT-TES-F/ADT-TIPS-CN composite suggest efficient energy transfer from ADT-TES-F to ADT-TIPS-CN. Therefore, it is possible that the slow component in the rise dynamics of the transient photocurrent in Fig. 7 is due to a multi-step process that involves excitation of ADT-TES-F, followed by energy transfer to ADT-TIPS-CN, which then slowly dissociates via the energetically favorable hole transfer back to ADT-TES-F, while the electron remains trapped on the ADT-TIPS-CN molecules. This spatial separation of the electron and hole would then account for the reduced

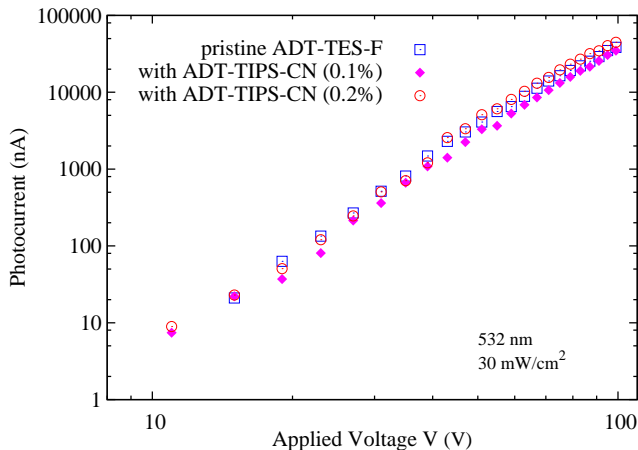


Figure 8. Photocurrent obtained in the pristine ADT-TES-F film and in ADT-TIPS-CN/ADT-TES-F films with 0.1% and 0.2% concentrations of the ADT-TIPS-CN on interdigitated Al electrodes (with 25 μm gap) as a function of applied voltage under cw 532 nm excitation at 30 mW/cm^2 .

probability of charge recombination, manifested through much slower photocurrent decay dynamics at long time-scales, as compared to pristine ADT-TES-F.

In all samples, cw photocurrent measured at light intensity of 30 mW/cm^2 was at least two orders of magnitude higher than the dark current. High bulk photoconductive gains of up to 130 have been previously reported in pristine ADT-TES-F films on Au electrodes under 0.58 mW/cm^2 532 nm cw excitation at average electric fields of 4×10^4 V/cm and attributed to long carrier lifetimes.⁵ These values are similar to those observed in GaN photodetectors²⁶ and at least an order of magnitude higher than those in unsubstituted pentacene and in most functionalized pentacene films.^{9,10} Under the same conditions, pristine ADT-TIPS-CN films showed a cw photoresponse weaker by several orders of magnitude,⁵ both due to a non-injecting nature of the Au/ADT-TIPS-CN contact²⁵ and amorphous nature of the ADT-TIPS-CN film.

In contrast to dramatic changes in PL properties of ADT-TES-F films upon addition of ADT-TIPS-CN molecules, the cw photocurrent remained unchanged up to at least 1% of the ADT-TIPS-CN in ADT-TES-F (Fig. 8). This suggests that the energy transfer between ADT-TES-F and ADT-TIPS-CN molecules, which is responsible for the observed changes in the PL response and in transient photocurrent, did not significantly affect equilibrium transport, at least at relatively low ADT-TIPS-CN concentrations. Currently, we are investigating the cw photocurrent behavior at higher concentrations of the guest molecules, which will be reported elsewhere.

4. CONCLUSIONS AND OUTLOOK

In summary, we presented photoluminescent and photoconductive properties of mixtures of ADT derivatives. Single exponential PL decays with lifetimes τ of ~ 9 and ~ 13 ns and PL quantum yields of 70% and 76% were observed in toluene solutions of pristine ADT-TES-F and ADT-TIPS-CN compounds, respectively. No interaction between ADT-TES-F and ADT-TIPS-CN molecules was observed in solution. In pristine films, bi-exponential decays were obtained, with an average lifetime of 2.2 ns and 0.4 ns in ADT-TES-F and ADT-TIPS-CN films, respectively. Already at 0.1% of ADT-TIPS-CN in ADT-TES-F, the PL response from a film was dominated by that of the ADT-TIPS-CN guest molecules. Much longer PL decays were observed in the ADT-TIPS-CN/ADT-TES-F composite films, compared to those in pristine films and solutions. Strong temperature dependence of the quantum yields, with a quantum yield reduction by a factor of 3–6 as the temperature increased from 5 $^\circ\text{C}$ to 80 $^\circ\text{C}$, was observed in films, but not in solutions. Blueshift of the peak fluorescence emission as the temperature increased was observed in ADT-TIPS-CN/ADT-TES-F mixtures, but not the pristine ADT-TES-F films. A slow component of charge photogeneration was introduced in the transient photocurrent dynamics in ADT-TIPS-CN/ADT-TES-F films, as compared to those in the pristine ADT-TES-F. The decay dynamics of the photocurrent in the composite film was also slower, which reflects reduced carrier recombination. No

considerable change in the cw photocurrent was observed upon adding of up to 1% of ADT-TIPS-CN molecules in the ADT-TES-F host at 532 nm excitation. Availability of several high-performance solution-processable derivatives such as the compounds considered here opens up new possibilities to tune optical and electronic properties of materials for specific applications by creating mixtures of various derivatives. An additional exciting development is that ADT-TES-F molecules can be imaged on a single-molecule level (using conventional wide-field fluorescence microscopy at 532 nm excitation) and yield characteristics comparable to those of fluorophores commonly utilized in single-molecule spectroscopy, such as DCDHF-N-6.¹² This allows one to study charge and energy transfer processes on the molecular level and relate them to the bulk material properties reported above. Such studies are currently underway.

5. ACKNOWLEDGEMENTS

We thank Dr. J. Day for assistance with transient photocurrent measurements and Profs. S. Rouvimov and P. Moeck for TEM characterization. This work was supported in part by the Office of Naval Research (grant #N00014-07-1-0457 via ONAMI Nanometrology and Nanoelectronics Initiative), and National Science Foundation via CAREER program (DMR-0748671).

REFERENCES

- [1] Forrest, S. R., "The path to ubiquitous and low-cost organic electronic appliances on plastic," *Nature* **428**, 911 (2004).
- [2] Day, J., Platt, A. D., Ostroverkhova, O., Subramanian, S., and Anthony, J. E., "Organic semiconductor composites: influence of additives on the transient photocurrent," *Appl. Phys. Lett.* **94**, 013306 (2009).
- [3] Ostroverkhova, O. and Moerner, W. E., "Organic photorefractives: mechanisms, materials and applications," *Chem. Rev.* **104**(7), 3267–3314 (2004).
- [4] Anthony, J. E., "Functionalized acenes and heteroacenes for organic electronics," *Chem. Rev.* **106**, 5028–5048 (2006).
- [5] Platt, A. D., Day, J., Subramanian, S., Anthony, J. E., and Ostroverkhova, O., "Optical, fluorescent, and (photo)conductive properties of high-performance functionalized pentacene and anthradithiophene derivatives," *J. Phys. Chem. C* (In Press).
- [6] Park, S. K., Mourey, D. A., Subramanian, S., Anthony, J. E., and Jackson, T. N., "High-mobility spin-cast organic thin film transistors," *Appl. Phys. Lett.* **93**, 043301 (2008).
- [7] Subramanian, S., Park, S. K., Parkin, S. R., Podzorov, V., Jackson, T. N., and Anthony, J. E., "Chromophore fluorination enhances crystallization and stability of soluble anthradithiophene semiconductors," *J. Am. Chem. Soc.* **130**, 2706 (2008).
- [8] Day, J., Subramanian, S., Anthony, J. E., Lu, Z., Twieg, R. J., and Ostroverkhova, O., "Photoconductivity in organic thin films: From picoseconds to seconds after excitation," *J. Appl. Phys.* **103**, 123715 (2008).
- [9] Gao, J. and Hegmann, F. A., "Bulk photoconductive gain in pentacene," *Appl. Phys. Lett.* **93**, 223306 (2008).
- [10] Lehnher, D., Gao, J., Hegmann, F. A., and Tykewinski, R. R., "Synthesis and electronic properties of conjugated pentacene dimers," *Org. Lett.* **10**(21), 4779–4782 (2008).
- [11] Lakowicz, J. R., [*Principles of Fluorescence Spectroscopy*], Springer, New York (2006).
- [12] Lord, S. J., Lu, Z., Wang, H., Willets, K. A., Schuck, P. J., Lee, H.-I. D., Nishimura, S. Y., Twieg, R. J., and Moerner, W. E., "Photophysical properties of acene DCDHF fluorophores: Long-wavelength single-molecule emitters designed for cellular imaging," *J. Phys. Chem. A* **111**, 8934–8941 (2007).
- [13] Ostroverkhova, O., Shcherbyna, S., Cooke, D. G., Egerton, R. F., Hegmann, F. A., Tykewinski, R. R., Parkin, S. R., and Anthony, J. E., "Optical and transient photoconductive properties of pentacene and functionalized pentacene thin films: Dependence on film morphology," *J. Appl. Phys.* **98**, 033701 (2005).
- [14] Como, E. D., Loi, M. A., Murgia, M., Zamboni, R., and Muccini, M., "J-aggregation in α -sexithiophene submonolayer films on silicon dioxide," *J. Am. Chem. Soc.* **128**, 4277–4281 (2006).
- [15] Troisi, A. and Orlandi, G., "Charge-transport regime of crystalline organic semiconductors: diffusion limited by thermal off-diagonal electronic disorder," *Phys. Rev. Lett.* **96**, 086601 (2006).

- [16] Troisi, A., Orlandi, G., and Anthony, J. E., "Electronic interactions and thermal disorder in molecular crystals containing cofacial pentacene units," *Chem. Mat.* **17**, 5024 (2005).
- [17] Clark, J., Silva, C., Friend, R. H., and Spano, F. C., "Role of intermolecular coupling in the photophysics of disordered organic semiconductors: aggregate emission in regioregular polythiophene," *Phys. Rev. Lett.* **98**, 206406 (2007).
- [18] Thorsmolle, V. K., Averitt, R. D., Densar, J., Smith, D. L., Tretiak, S., Martin, R. L., Chi, X., Crone, B. K., Ramirez, A. P., and Taylor, A. J., "Morphology effectively controls singlet-triplet exciton relaxation and charge transport in organic semiconductors," *Phys. Rev. Lett.* **102**, 017401 (2009).
- [19] Kobitski, A. Y., Scholz, R., Zahn, D. R. T., and Wagner, H. P., "Time-resolved luminescence study of excitons in α -PTCDA as a function of temperature," *Phys. Rev. B* **68**, 155201 (2003).
- [20] Kishore, V., Narasimhan, K. L., and Periasamy, N., "On the radiative lifetime, quantum yield and fluorescence decay of Alq in thin films," *Phys. Chem. Chem. Phys.* **5**, 1386–1391 (2003).
- [21] Harrison, N. T., Baigent, D. R., Samuel, I. D. W., Friend, R. H., Grimsdale, A. C., Moratti, S. C., and Holmes, A. B., "Site-selective fluorescence studies of poly(*p*-phenylene vinylene) and its derivatives," *Phys. Rev. B* **53**(23), 15815–15822 (1996).
- [22] Guha, S., Rice, J. D., Yau, Y. T., Martin, C. M., Chandrasekhar, M., Chandrasekhar, H. R., Guentner, R., de Freitas, P. S., and Scherf, U., "Temperature-dependent photoluminescence of organic semiconductors with varying backbone conformation," *Phys. Rev. B* **67**, 125204 (2003).
- [23] Mikhnenko, O. V., Cordella, F., Sieval, A. B., Hummelen, J. C., Blom, P. W. M., and Loi, M. A., "Temperature dependence of exciton diffusion in conjugated polymers," *J. Phys. Chem. B* **112**(37), 11601 – 117604 (2008).
- [24] Rebarz, M., Wojdyla, M., Bala, W., and Lukasiak, Z., "Study of excited states in thin films of perylene derivatives by photoluminescence and absorption spectroscopy," *Opt. Mat.* **30**(5), 774 – 776 (2008).
- [25] Day, J., Platt, A. D., Subramanian, S., Anthony, J. E., and Ostroverkhova, O., "Influence of organic semiconductor-metal interfaces on the photoresponse of functionalized anthradithiophene thin films," *J. Appl. Phys.* **105**, 103703 (2009).
- [26] Munoz, E., Monroy, E., Garrido, J. A., Izpura, I., Sanchez, F. J., Sanchez-Garcia, M. A., Calleja, E., Beaumont, B., and Gibart, P., "Photoconductor gain mechanisms in GaN ultraviolet detectors," *Appl. Phys. Lett.* **71**, 870–872 (1997).